JOURNAL OF OPTOELECTRONICS AND ADVANCED MATERIALS Vol. 9, No. 6, June 2007, p. 1821 - 1824

IR and thermal studies of iron oxide nanoparticles in a bioceramic matrix

C. BIRSAN*, D. PREDOI[a], E. ANDRONESCU
University "Politehnica" of Bucharest, Faculty of Applied Chemistry and Materials Science, Department of Science and Engineering of Oxide Materials and Nanomaterials 1 – 7, Polizu Street, 011061, PO – BOX 12-134 Bucharest 1, Romania
[a]National Institute for Physics of Materials, P.O. Box. MG 07, 077125, Bucharest-Magurele, Romania

Magnetic iron oxide nanoparticles have a great potential in various applications in biomedical research and technology. Iron oxide particles such as magnetite (Fe_3O_4) is by far the most commonly employed magnetic materials for biomedical applications. Bioceramic composites were obtained by combining the magnetite with two biocompatible components (hydroxyapatite and bioglass). Their thermal behaviour has been studied by thermal analysis (DTA and TG). The interaction of iron oxide with the bioceramic matrix has been investigated using IR spectroscopy.

(Received November 14, 2006; accepted April 26, 2007)

Keywords: Magnetic bioceramic, IR spectroscopy, Thermal analysis, Iron oxide nanoparticles

1. Introduction

The magnetic bioceramics are being studied for their current and future applications in medicine and biology including the treatment of the bone cancer [1], magnetic resonance imaging contrast enchancement [2-5], magnetic transport of anti cancer drugs [6-9], hyperthermia [10-12]. Even though the classic method involves magnetite, late scientific references emphasize superior results by using maghemite ($\gamma - Fe_2O_3$) or nanometric magnetite, which show remarkable new phenomena such as superparamagnetism [13]. The properties of magnetic bioceramics depend on the particles size, the particles-bioceramic matrix interactions and the degree of dispersion of the nanoparticles in the matrix [14-16].

The aim of this paper was the synthesis of bioceramic composites with ferromagnetic properties using an unconventional method, as well as their characterization using X-ray diffraction, Scanning Electron Microscopy (SEM), IR spectrometry, DTA (diferential thermal analysis) and TG (thermal gravimetry) analysis.

2. Experimental

Sample preparation

In order to obtain a ceramic biocomposite with possible applications in the bone cancer treatment, the excellent biocompatibility properties of two materials (hydroxyapatite (HAp) and a bioglass (BG) with the composition 23.5%CaO, 47% SiO_2, 23.5% Na_2O and 6% P_2O_5) and the magnetic properties of magnetite, were considered. Three different compositions were chosen as presented in the Table 1. The raw materials used for the bioglass synthesis ($CaCO_3$, SiO_2, $Na_2CO_3{*}10H_2O$, $NH_4)_2HPO_4$ were milled for 1h at 180 rot / min, melted at 1400^0C and then cooled fast in the water. The as obtained glass was milled for 5 hours at 180 rot / min, in the presence of ethanol. The resulting powder had a specific surface area of 3.87 m^2/cm^3 and the average diameter of the grains was 2.728 μm.

Table 1. The composition of the three ceramic biocomposite samples.

Sample	HAp (weight %)	Bioglass (weight %)	Fe_3O_4 (weight %)
M1	32.5	32.5	35
M2	65	0	35

The hydroxyapatite, bioglass and commercial magnetite powders were milled for 1h at 180 rot / min. in a dried environment and then DTA / TG and IR studies were performed on the powders.

Sample characterization

The samples were characterized by X-ray diffraction (XRD) with a Philips PW1050 X-ray powder diffractometer using CuK_α incident radiation. An estimation of crystallite sizes was made from the diffraction line width and using the Scherrer formula. The structure and morphology of the powder samples have been studied using a HITACHI S2600N type Scanning Electron Microscope (SEM) coupled with an EDAX (Energy Dispersive X-Ray Analysis) device, operating at 25kV in vacuum.

The IR absorption spectra were performed in the 1800 to 400 cm^{-1} range using a BX FT-IR spectrophotometer.

The measurements were carried on dehydrated powdered samples embedded in KBr pellets. Differential Thermal Analysis (DTA) and Thermal Gravimetric (TG) analysis were performed using a Shimadzu DTG-TA-50 and DTA 50 analyser, in the 25 – 1000 ^{o}C temperature range, weight detection ±20- ± 200 mg, in open air and using Al_2O_3 as reference.

3. Results and discussions

Fig. 1 shows the X-ray diffraction (XRD) patterns (Fig. 1a) and SEM image showing the morphology of commercial magnetite powder (Fig. 1b).

The X ray diffraction (XRD) patterns shows peaks corresponding to a cubic spinel structure. The analysis of the crystallite size (D) of the maghemite and bioceramics phases has been dined for all samples using the Scherrer's equation [17]:

$$D = \frac{K\lambda}{B\cos\theta}$$

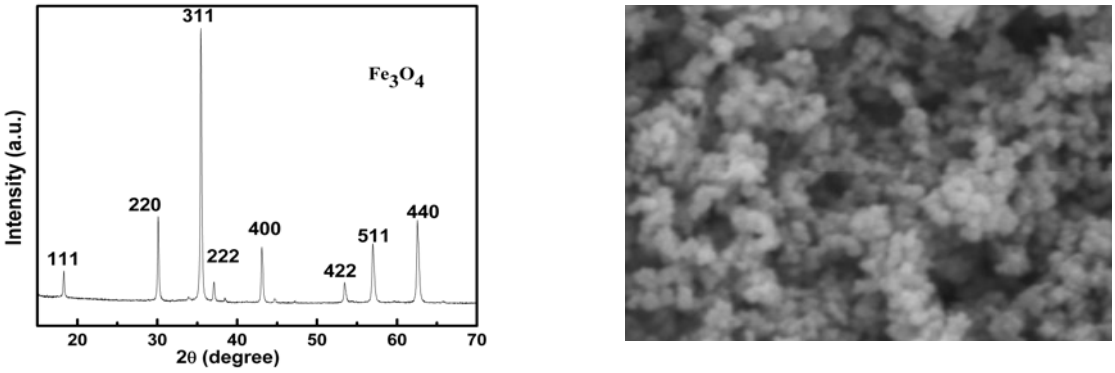

Fig. 1. X-Ray diffraction pattern of commercial Fe_3O_4 (left side) and SEM image of commercial magnetite powder (right side).

The SEM image of the commercial magnetite powder exhibit particles that have the sizes in the 0.8 to 2 μm range which are in a good agreement with the particles sizes calculated using the XRD patterns <D>=1 μm.

The XRD patterns of the commercial HAp and commercial HAp with commercial Fe_3O_4 addition (M1) and HAp with bioglass and magnetite addition (M2) are shown in Fig. 2. Fig. 2 shows the peaks corresponding to crystalline hydroxyapatite and to a cubic spinel structure.

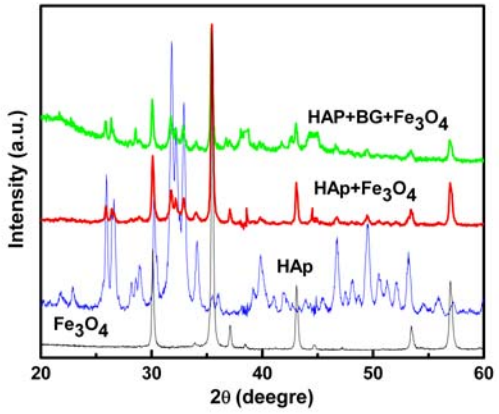

Fig. 2. X-Ray diffraction pattern of commercial HAp and samples M1 and M2.

Thermal analyses of commercial magnetite carried out using simultaneous TG and DTA measurements are shown in Fig. 3. DTA curve analysis showed that water was removed below 200 ^{o}C (DTA endothermic peak). The conversion of magnetite (Fe_3O_4) into maghemite (γ-Fe_2O_3) take place around 330 ^{o}C (DTA exothermic peak). The gradual decrease in weight from 400 ^{0}C to 1000 ^{0}C is probably a result of the show elimination of the carbonate groups linked to HAp, the presence of which has been confirmed by FTIR analysis discussed later [20]. The differences in weight loss of sample M1 and sample M2 shows that the weight loss is determinate by bioglass addition.

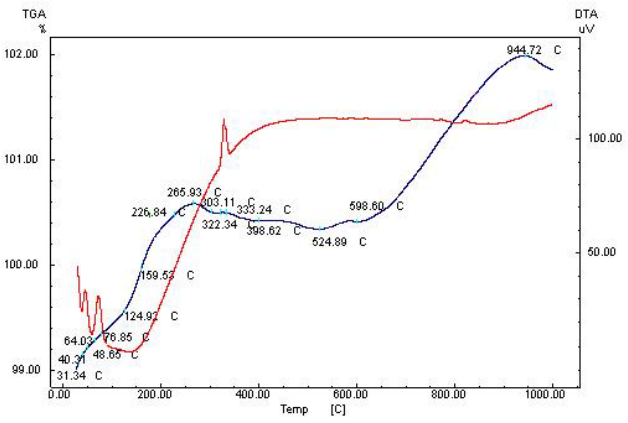

Fig. 3. The DTA/TGA evolution curves for the commercial magnetite powder.

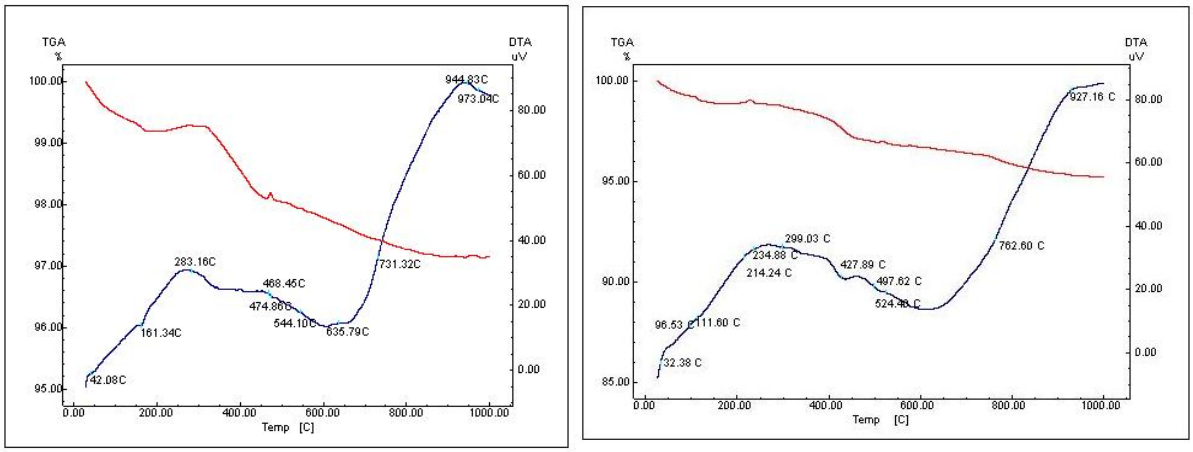

Fig. 4. The DTA/TGA evolution curves for M1(left) and M2(right) samples.

Fig. 4 shows the DTA/TGA measurements performed on the M1 (a) and M2 (b) samples. The weight loss between 100 ^{0}C and 450 ^{0}C contributes to the loss of lattice water [18-19]. The study results emphasize the $Fe_3O_4 \rightarrow \gamma$–$Fe_2O_3$ transformation in the temperature range 300-400 ^{0}C. The temperature of this transformation depends on the sample composition – the weight increase due to this change is smaller for M2 and higher for M1. The hydroxyapatite content has also an influence on this transformation, diminishing the amount of transformed magnetite.

In the Fig. 5 the IR absorption spectra of the raw materials (Fe_3O_4, HAp and BG) and the two prepared samples (M1 and M2), are shown. Since magnetite has an inverse spinel type structure, it shows characteristic vibration bands: M_{Th}-O-M_{Oh} (ν1≈ 600-550 cm^{-1}), M_{Oh}-O (ν2≈ 470 cm^{-1}) and M_{Th}-M_{Oh} (ν3≈ 350-400 cm^{-1}), where M_{Th} and M_{Oh} correspond to the metal occupying tetrahedral and octahedral positions respectively [21-22]. The stretching vibration ν (Fe-O) correspond of tetrahedral iron atoms. The band at 3500 cm^{-1} and the bands at 1640 cm^{-1} is due to the vibrations of hydrogen-bonded water molecules adsorbed on the surface [23].

Prominent HAp bands include the ν4 O-P-O bending bands at 565 cm^{-1} and the OH librational band at 630 cm^{-1} [24]. Bending bands of HAp at 600 cm^{-1} and 594 cm^{-1} which are attributed to the PO_4^{3-} ions (ν_4) merge to form a strong band at 597 cm^{-1} which disappears with bioglass adition. The next most prominent HAp band is the 1040 cm^{-1} (ν3) band which is attributed to the PO_4^{3-} ions [25] and decreases with the addition of bioglass. For PO_4^{3-} group the characteristic vibration are ν_4 vibration (asymmetric bending) at 600 cm^{-1}, ν_1 vibration (symmetric stretching) at 962 cm^{-1}, and a set of peaks in the 1000-1200 cm^{-1} region assigned to the ν_3 vibrations mode (asymmetric stretching). For CO_3^{-2} groups, two bands at 1415 and 1467 cm^{-1} of the ν_3 vibrations mode (asymmetric stretching) and a small peak at 875 cm^{-1} corresponding to ν_2 vibration (asymmetric stretching) have been observed. The presence of the peaks in the commercial sample indicates carbon as in impurity introduced during preparation process.

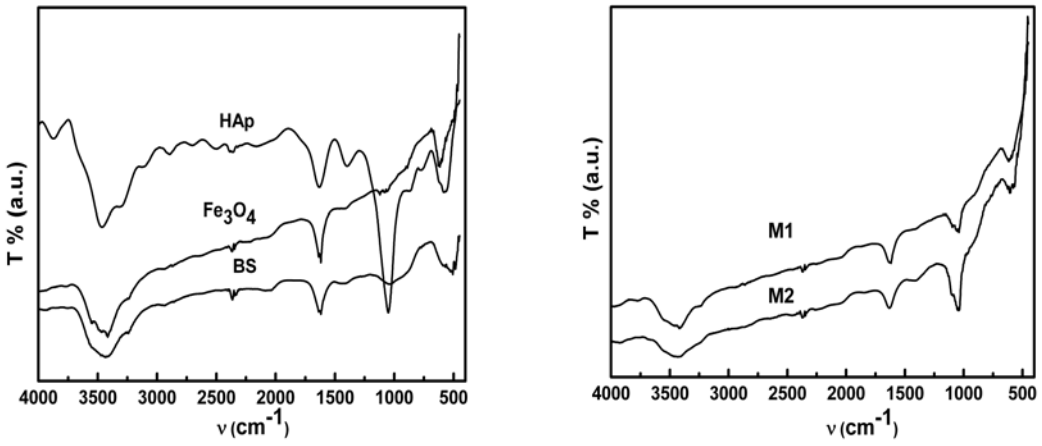

Fig. 5. FTIR spectra of the raw materials (Fe_3O_4, HAp and BG) and of the samples M1 and M2.

For the BS and M1 samples the 685 cm^{-1} band was observed and identified in α–quartz [26]. The 800 cm^{-1} band has been associated with O-Si-O bending in colloidal silica [27], while the 870 cm^{-1} band was identified as ν_3 Si-O stretching band in silicates [28]. For all samples the broad bands attributed to absorbed water were also observed at 3440 cm^{-1} and 1620 cm^{-1}. The absorbed water band exists up to 300 ^{0}C, which indicate that the continued weight loss observed in the thermal analysis is due to lattice-absorbed water.

4. Conclusions

Bioceramic composites were obtained by combining the magnetite with two biocompatible components (hydroxyapatite and bioglass). The experimental results emphasized that the grain size of the powder and the type of the biocomponent (hydroxyapatite or bioglass) have a great influence on the ability of magnetite to transform into maghemite and haematite.

Acknoledgements

This work was supported by the National Romanian Research Program grants (CEEX_24/2005 VIASAN Program)

References

[1] D. Bahadur, Jyotsnendu Giri, Biomaterials and magnetism, Sadhana **28**, Parts 3 & 4, June/August, 639–656 (2003).
[2] M. Ikenaga, K. Ohura, T. Nakamura, Y. Kotoura, T. Yamamuro, M. Oka, Y. Ebisava, T. Kokubo, Bioceramics **4**, 255 (1991).
[3] K. Ohura, M. Ikenaga, T. Nakamura, T. Yamamuro, Y. Ebisava, T. Kokubo, Y. Kotoura, M. Oka, J. Appl. Biomat **2**, 159 (1991).
[4] T. Kokubo, Y. Ebisava, Y. Sugimoto, M. Kiyama, K. Ohura, T. Yamamuro, M. Hiraoka, M. Abe, Bioceramics **5**, 213 (1992).
[5] Th. Leventouri, A. C. Kis, J. R. Thompson, I. M. Anderson, Biomaterials **26**, 4924 (2005).
[6] M. Jesús de la Fuente and Soledad Penadés, Biochimica et Biophysica Acta (BBA), **1760**(4), 636 (2006).
[7] P. Tartaj, M. P. Morales, T. González-Carreño, S. Veintemillas-Verdaguer, C. J. Serna, J. Magn. Magn. Mater. **290-291**, part 1, 28 (2005).
[8] Masashige Shinkai, Journal of Bioscience and Bioengineering **94**, 606 (2002).
[9] Yong-Min Huh and Young Jin Kim, Current Applied Physics in Press, 2006.
[10] M. Ikenaga, K. Ohura, T. Yamamuro, Y. Kotoura, M. Oka, T. Kokubo, J. Orthop. Res. **11**, 849 (1993).
[11] Y. Ebisava, F. MiYaji, T. Kokubo, K. Ohura, T. Nakamura, J. Biomater **18**, 1277 (1997).
[12] K. Takegami, T. Sano, H. Wakabayashi, J. Sodona, T. Yamazaki, S. Morita, T. Shibuya, A. Uchida, J. Biomed. Mater. Res. **43**, 210 (1998).
[13] D. H. Kim, S. H. Lee, K. H. Im, K. N. Kim, K. M. Kim, I. B. Shim, M. H. Lee, Y. K. Lee, Current Applied Physics, In Press, 2006.
[14] M. A. McDonald, K. L. Watkin, Academic Radiology **13**, 421 (2006).
[15] E. Illés, E. Tombácz, Journal of Colloid and Interface Science **295**, 115 (2006).
[16] E. De Biasi, C. A. Ramos, R. D. Zysler, D. Fiorani, Physica B: Condensed Matter **372**, 345 (2006).
[17] R. M. Cornell, U. Schertmann, Iron Oxides in the Laboratory: Preparation and Characterisation, VCH, Weinheim, 1991.
[18] W. Suchanek, Y. Masahiro, J. Mater. Res. **13**(1), 94 (1998).
[19] W. L. Suchanek, P. Shuk, K. Byrappa, R. E. Riman, K. S. Tenhuisen, V. F. Janas, Biomaterials **23**, 699 (2002).
[20] P. N. Kumta, C. Sfeir, D. H. Lee, D. Olton, D. Choi, acta Biomaterialia **1**, 65 (2005).
[21] E. Barrodo, F. Prieto, J. Medina, F. A. Lopez, J. Alloys. Compd. **335**, 203 (2002).
[22] J. L. Martin de Vidales, A. Lopez-Delgado, E. Vila, F. A. Lopez, J. Alloys. Compd. **287**, 276 (1999).
[23] M. L. Hair, J. Non-Cryst. Solids **19**, 299 (1975).
[24] K. C. Blakesee, Sr. R. A. Condrate, J. Am. Ceram.Soc. **54**, 559 (1971).
[25] A. Jillavencatesa, Sr. R. A. Condrate, Spectrosc. Lett. **31**, 1619 (1988).
[26] R. K. Sato, P. F. McMillan, J. Phys. Chem. **91**, 3494 (1987).
[27] C. Hollenstein, A. A. Howling, C. Courteille, D. Magni, S. M. Scholz, G. M. W. Kroesen, J. Phys. D, Appl. Phys. **31**, 74 (1998).
[28] J. Etchepar, Spectro. Acta A Mol Spectrosc. **26**, 2147 (1970).

*Corresponding author: birsan_1@yahoo.com